Hybrid Control Based on Backstepping Sliding Mode Control for Flow Modulation of Electric Fuel Pump

Han Zhang[1], Bin Wang[2][a], Zhifeng Ye[2], Tengfei Ma[1] and Hongcheng Zhang[1]

[1]College of Energy and Power Engineering,
Nanjing University of Aeronautics and Astronautics, Nanjing 210016, China
[2]Jiangsu Province Key Laboratory of Aerospace Power System,
Nanjing University of Aeronautics and Astronautics, Nanjing 210016, China

Keywords: Electric Fuel Pump, Flow Modulation, Hybrid Control, Fault-Tolerant.

Abstract: As the core component of more electric engine (MEE), electric fuel pump is composed of a permanent magnet synchronous motor (PMSM) integrated with a high-pressure gear pump. Rotation speed is controlled by the motor and the pump discharges the fuel with required amount into the engine combustor. How the speed control system works largely determines the delivery flow rate of the pump, although delivery pressure can disturb the flow rate as well. Hence, it must be capable of delivering the maximum needed flow at appropriate pressure to obtain satisfactory nozzle spray and accurate fuel regulation. In order to improve modulation performance of the electric fuel pump with all conditions accessible, a complete mathematical model of the pump is built and the hybrid control strategy within the scope of whole operation is proposed, considering the measured parameter of fuel flow as feedback. The control strategy consists of a feed-forward compensation based on differential pressure and backstepping non-singular fast terminal sliding mode control with extend state observer. Results show that the hybrid control strategy can meet the requirements of fuel flow regulation for aeroengines including accuracy of wide range flow and quick response ability. Additionally, the effectiveness of redundancy design is shown, which contributes to its reliability as an airborne component.

1 INTRODUCTION

The More Electric Engine, incorporating new advances in motor/generators, active magnetic bearings, power electronics and other electrical technologies (Mohammadi et al., 2021; Wang et al., 2021; McLoughlin et al., 2009), has attracted wide attention with its excellent properties including reduced specific fuel consumption, high thrust-weight ratio, reliability, maintainability, and environmental friendliness.

Nowadays, the main fuel pump of aero-engine generally adopts a gear pump, which has the advantages of large flow rate, compact configuration, and high reliability (Morioka et al., 2013). It is a type of constant displacement pump which delivers a continuous supply of fuel at the proper pressure. However, the speed of pump is proportionally related to engine speed so that the flow is unable to be independently regulated. Consequently, the delivered fuel flow rate can be several times greater than the amount the engine requires, so the fuel return arrangement is indispensable in a traditional fuel system. Power loss and fuel temperature rising are exacerbated due to the large amount of pressurized fuel return, which may pose a potential threat to the performance and even safety of the engine.

On the contrary, as one of the core components of MEE, electric fuel pump is driven by a fault-tolerant electric motor rather than conventional AGB (Accessory Gear Box) (Newman, 2004), so that the system can be individually controlled to deliver the exact fuel flow demanded by the engine. Hence, it must be capable of delivering the flow at appropriate pressure required for satisfactory fuel atomization and accurate fuel regulation. Therefore, the flow modulation of electric fuel pump is an essential issue.

The electric fuel pump is composed of a permanent magnet synchronous motor integrated

---

[a] https://orcid.org/0000-0002-5809-616X

with a gear pump. Compared with conventional counterparts, the electric fuel pump can not only improve the system efficiency and the flexibility of variable speed control but also reduce the weight and volume of the airborne fuel system.

Many researches on the electric motors or pumps for MEE have been conducted to date. The following reviews some of them. In (Jiang et al., 2015), a new electric drive system based on a six-phase ten-pole dual-winding fault-tolerant permanent magnet (DFPM) motor was proposed and investigated. It is a potential power unit in aerospace due to its high reliability and strong fault tolerance. Based on an assumed small-sized turbofan engine, Morioka N conducted a rig testing of the proposed MEE electric fuel system using experimental hardware and bench set-up. He adopted a fuel-flow feedback system for the required metering accuracy (Morioka et al.,2014). Similarly, a robust control method based on combined sliding mode control surface which applies to the electric fuel pump is proposed (Ding et al., 2019). Equations of the flow characteristics of an electric gear fuel pump were developed by applying the improved BP neural network (Liu et al., 2020).

Less in-depth research on control strategies of fuel flow has been conducted. To achieve accurate flow control of the electric fuel pump, this paper proposes a hybrid control strategy. The hybrid fuel flow control strategy consists of a feed-forward compensation based on differential pressure and backstepping non-singular fast terminal sliding mode control with extend state observer. Simulations with the proposed control strategy in terms of flow modulation are conducted and the results are compared with the results of using ADRC and SMC. Besides, considering the possible fault of the motor during the operation of the electric fuel pump, the simulation of the motor open circuit fault was carried out.

2 MATHEMATICAL MODEL

2.1 DFPMSM

A six-phase ten-pole dual-winding fault-tolerant permanent magnet motor (DFPMSM) is employed to drive the fuel gear pump. PMSM converts electrical energy into mechanical energy. Inducing electromagnetic torque through the current/coil interaction, it drives the gear pump. The dynamics

model of the DFPMSM mainly comprises the voltage equation, the electromagnetic torque equation, and the motion equations.

$$
\begin{bmatrix} U_{d1} \\ U_{q1} \end{bmatrix} = \begin{bmatrix} R + pL_{d1} & -\omega_e L_{q1} & p\varphi_f \\ \omega_e L_{d1} & R + pL_{q1} & \omega_e \varphi_f \end{bmatrix} \begin{bmatrix} i_{d1} \\ i_{q1} \\ 1 \end{bmatrix} \tag{1}
$$

$$
\begin{bmatrix} U_{d2} \\ U_{q2} \end{bmatrix} = \begin{bmatrix} R + pL_{d2} & -\omega_e L_{q2} & p\varphi_f \\ \omega_e L_{d2} & R + pL_{q2} & \omega_e \varphi_f \end{bmatrix} \begin{bmatrix} i_{d2} \\ i_{q2} \\ 1 \end{bmatrix} \tag{2}
$$

where U_{d1} and U_{q1} are the d-q-axis voltages of the ABC winding while U_{d2} and U_{q2} are the d-q-axis voltages of the UVW winding, $R=diag[R_s\ R_s\ R_s]^T$ is the stator resistance, p is the differential operator, ω_e is the electrical angular speed of the rotor, $\omega_e=n\omega_r/2$, ω_r is the mechanical angular speed of the rotor and n is the pole pair number of the motor, L_{d1} and L_{d2} are the stator inductance vector on d-axis of the ABC winding and the UVW winding respectively, L_{q1} and L_{q2} are the stator inductance vector on q-axis of the ABC winding and the UVW winding respectively, i_{d1} and i_{q1} are the d-q-axis currents of the *ABC* winding while i_{d2} and i_{q2} are the d-q-axis currents of the UVW winding, φ_f is the magnetic flux linkage.

The electric torque T_e can be written as

$$
T_e = \frac{3}{2}\frac{n}{2}\left\{ \begin{bmatrix} \varphi_f i_{q1} + (L_{d1} - L_{q1}) i_{d1} i_{q1} \end{bmatrix} \\ + \begin{bmatrix} \varphi_f i_{q2} + (L_{d2} - L_{q2}) i_{d2} i_{q2} \end{bmatrix} \right\} \tag{3}
$$

According to the structural characteristics of surface-mounted PMSM, $L_{d1}=L_{q1}$, $L_{d2}=L_{q2}$, T_e can be simplified as

$$
T_e = \frac{3}{2}\frac{n}{2}\varphi_f\left(i_{q1} + i_{q2}\right) = \frac{3}{2}\frac{n}{2}\varphi_f i_q \tag{4}
$$

The dynamics of the rotor can be expressed by

$$
J\frac{d\omega_r}{dt} = T_e - T_L - B_0\omega_r \tag{5}
$$

2.2 Gear Pump

Owing to simple structure, lightweight, and better-uncontaminated ability, external gear pump is frequently used in aero fuel systems (Rundo, 2017).
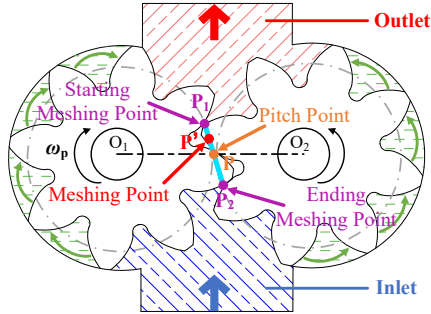

Figure 1: Gear pump meshing schematic.

Figure 1 shows the meshing schematic of the gear pump. Based on operation principle and flow continuity assumption, the instantaneous flow rate of a gear pump is

$$Q_v = B\omega_p \left(2R_c h + h^2 - f^2\right) = B\omega_p \left(R_a^2 - R_c^2 - f^2\right) \quad (6)$$

where R_a and R_c are the radius of the addendum and the pitch circles, respectively, ω_p is the angular velocity of the pump, f is the distance between the meshing point P' and the pitch point P.

The internal leakage of gear pump is inevitable especially those which deliver high-pressure fluid. Leakage flow includes two parts of axial and radial clearance leakage (Chen, et al., 2018).

The total leakage can be expressed by

$$Q_s = 4\left[\frac{(\theta_b + \theta_h)\,s^3 \Delta p}{12\mu \ln\left(R_b / R_z\right)} + \frac{(2\theta_b + \theta_h)\,\rho \omega_p^3 s^3 \left(R_b^2 - R_z^2\right)}{80\mu \ln\left(R_b / R_z\right)}\right] \quad (7)$$

$$Q_\delta = B\left(\frac{\Delta p \delta^3}{6\mu S_e Z_0} - \frac{1}{30}\pi n_p R_a \delta\right) \quad (8)$$

where Q_s and Q_δ are the axial and radial clearance leakage respectively. R_b is the root radius, R_z is the radius of the gear shaft, θ_h is the wrap angle of the high-pressure cavity, θ_b is the half wrap angle within the transition zone, s is the axial clearance, δ is the radial clearance, μ is the kinetic viscosity which is vulnerable to the temperature of the fluid, B is the face width, S_e is the crest width, Z_0 is the number of the teeth in transition zone, n_p is the rotation speed of the pump.

Thus, the real flow rate can be written as

$$Q = Q_v - Q_l = Q_v - (Q_s + Q_\delta) \quad (9)$$

There is no doubt that the real flow rate is not only determined by rotation speed but also depends on the differential pressure and the fuel temperature. These factors bring system uncertainties and impair pump accuracy. Moreover, to obtain a complete model of the PMSM, it is necessary to describe the dynamic torque of the gear pump. A gear pump with unloading groove is modelled.

For the driven gear,

$$\begin{cases} M_{2n} = F_n R_b \\ M_{2o} = S_{ak}\Delta p B R_b \\ M_{2o} = M_{2n}\eta_{m2} \end{cases} \quad (10)$$

F_n is the engaging force of two gears, so it can be expressed as

$$F_n = \frac{S_{ak} B \Delta p}{\eta_{m2}} \quad (11)$$

Similarly, for the driving gear,

$$\begin{cases} M_{1n} = F_n R_b \\ M_{1o} = S_{ck}\Delta p B R_b \end{cases} \quad (12)$$

M_{1n}, the torque on the driving gear plus the torque generated by the fuel in the tooth groove balances with the product of the system input torque M and its mechanical efficiency η_{m1}.

$$M\eta_{m1} = M_{1o} + M_{1n} \quad (13)$$

$$M = \frac{S_{ck}\Delta p \mathrm{B} R_b}{\eta_{m1}} + \frac{S_{ak}\Delta p B R_b}{\eta_{m1}\eta_{m2}} \quad (14)$$

The length of an involute tooth profile is (Li, et al., 2006)

$$S_{ak} = \frac{1}{2} R_b (\tan^2 \alpha_\alpha - \tan^2 \alpha_{k2}) \quad (15)$$

$$S_{ck} = \frac{1}{2} R_b (\tan^2 \alpha_\alpha - \tan^2 \alpha_{k1}) \qquad (16)$$

Substituting Eq. (15) and Eq. (16) into Eq. (14) yields:

$$M = \frac{BR_b^2 \Delta p}{2} \left(\frac{\tan^2 \alpha_a - \tan^2 \alpha_{k2}}{\eta_{m1}} + \frac{\tan^2 \alpha_a - \tan^2 \alpha_{k1}}{\eta_{m1}\eta_{m2}} \right) \qquad (17)$$

where α_a is the pressure angle of the tip circle, α_{k1} and α_{k2} are respectively the pressure angle of the driving and the driven gear at the meshing point, γ_{k1} and γ_{k2} are the central angle corresponding to the meshing point.

3 CONTROLLER DESIGN

Involving the PMSM and a gear pump, model uncertainties and unavoidable disturbances are inherent issues for an electric fuel pump under all conditions. The established mathematical pump model can only describe the input-output relationship, but there still exist certain operational uncertainties. For example, increasing sealing clearance due to wear and tear, cavitation due to high rotation speed or low inlet pressure, brings about the uncertainty, which cannot be fully accounted for in the modelling. Besides, PMSM is a typical multi-variable and strongly-coupled system, which is often disturbed by various uncertainties such as the external uncertain loads, the internal non-constant friction, and the nonlinear magnetic field effects. Its operation highly affects the performance of flow control. In addition, considering that the output of the turbine flowmeter is a frequency signal, either through the circumferential method or frequency measurement method of its output processing is unable to guarantee the accuracy and dynamic performance of the flow signal. It is difficult to achieve accurate and rapid feedback of fuel flow.

Therefore, a fuel flow hybrid control strategy is proposed. It consists of a feed-forward compensation based on differential pressure and backstepping non-singular fast terminal sliding mode control with extend state observer.
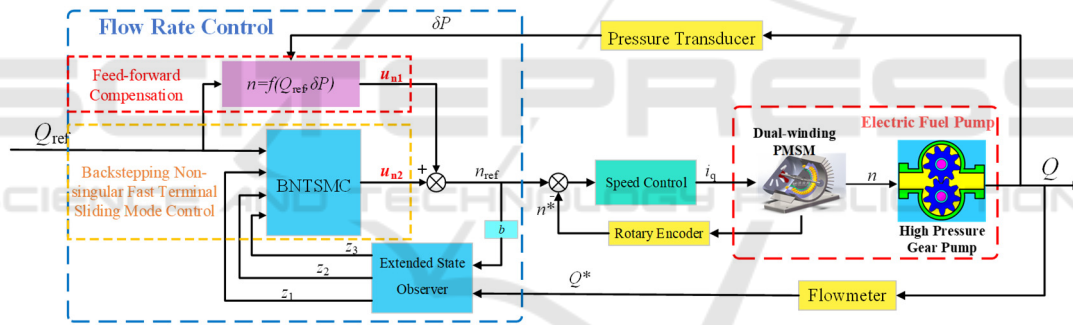

Figure 2: Schematic diagram with fuel flow hybrid control.

3.1 Feed-Forward Compensation Based on Differential Pressure

In order to obtain the relationship between flow rate and rotation speed of the electric fuel pump, a prototype pump is manufactured and tested. Figure 3(a) depicts the experimental system. Two pressure transducers and a flowmeter were adopted to collect the required pressure and fuel flow respectively.

Figure 3(b) depicts the comparison between the tested data and the fitted data. The root mean squared errors (RMSE) of the fitted curve is less than 0.5 under varied operating conditions, suggesting that the fitted curve can well represent the flow-speed-outlet pressure relationship of a prototype electric fuel pump.

According to the tested data shown in Figure 3(b), the relationship between rotation speed and flowrate can be obtained, which is also the input of the flow controller.

$$u_{n1} = f(Q_{ref}, \delta P) \qquad (18)$$
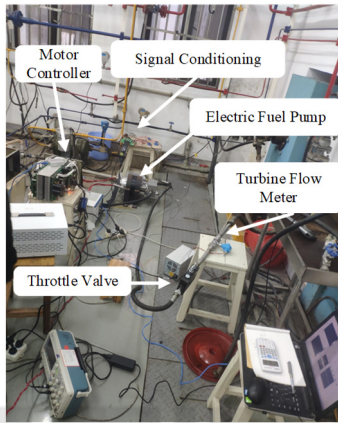
3.2 Liner Extended State Observer

According to the input and the output of the controlled object, a well-designed ESO can estimate the total disturbance on the system (Han, 2002; Gao, 2003).

A second-order system is used to mathematically characterize the electric fuel pump as

$$\begin{cases} \dot{Q} = \gamma \\ \dot{\gamma} = f(\gamma, a, b) + bn + \omega(t) \\ u = n \\ y = Q \end{cases} \tag{19}$$

$$\begin{cases} \dot{z}_1 = z_2 - 3\omega_0(z_1 - y) \\ \dot{z}_2 = z_3 - 3\omega_0^2(z_1 - y) + bu_n \\ \dot{z}_3 = -\omega_0^3(z_1 - y) \end{cases} \tag{20}$$

where $\omega(t)$ is the external interference and $f(\gamma, a, b)$ is the internal disturbance, the rotation speed n and the flow rate Q are the input and output of the electric fuel pump respectively.
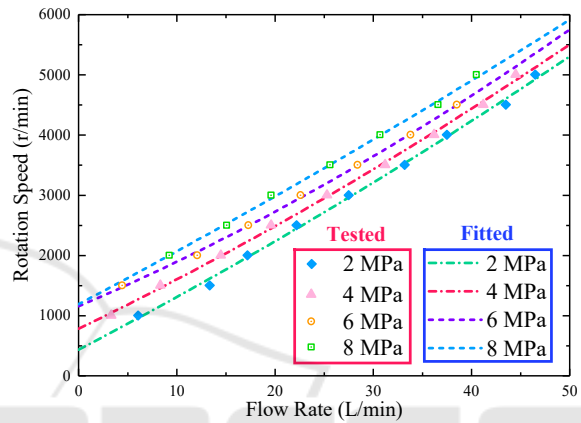
The following extended state observer is designed based on the model of electric fuel pump system:

where z_1 and z_2 is, respectively, the observation value and its differential of the flow rate; z_3 is the estimated value of the disturbance.

(a) Experimental system

(b) Comparison between tested data and fitted results

Figure 3: Experimental system and results.

3.3 Backstepping Non-Singular Fast Terminal Sliding Mode Control

The basic idea of the backstepping control method is to decompose the complex nonlinear system into subsystems that do not exceed the system order, and then design Lyapunov functions and intermediate virtual control variables for each subsystem, push the subsystem back to the whole system, and integrate them to complete the design of the whole control law.

Lemma 1: If the Lyapunov function $V(t,x)$ is positive definite, and $\dot{V} \leq -k_1 V + k_2$, k_1 and k_2 are bounded constants, which $k_1, k_2 \geq 0$, then

$$V(t,x) \leq \frac{k_2}{k_1} + \left[V(0) - \frac{k_2}{k_1} \right] e^{-k_1 t} \tag{21}$$

The fuel flow tracking error is defined as

$$\begin{cases} e_1 = Q - Q_d \\ \dot{e}_1 = \dot{Q} - \dot{Q}_d = \gamma - \dot{Q}_d \end{cases} \tag{22}$$

Take the virtual control as

$$\alpha_1 = -c_1 e_1 + \dot{Q}_d \tag{23}$$

According to the design process of the backstepping method, α_1 will be derived, but multiple derivations will increase the number of terms in α_1. Therefore, a first-order low-pass filter is employed to filter the virtual control values, which simplifies the parameters and structure of the final control method.

Take $\overline{\alpha}_1$ as the output of the low-pass filter of α_1

$$\begin{cases} \overline{\alpha}_1 = -c_1 e_1 + \dot{Q}_d \\ \tau \dot{\alpha}_1 + \alpha_1 = \overline{\alpha}_1 \\ \alpha_1(0) = \overline{\alpha}_1(0) \end{cases} \tag{24}$$

The error of resulting filter is

$$L = \overline{\alpha}_1 - \alpha_1 \tag{25}$$

Combining Eq. (24), the derivative of L is as follows:

$$\dot{L} = \dot{\bar{\alpha}}_1 - \dot{\alpha}_1 = \dot{\bar{\alpha}}_1 - \frac{L}{\tau} \qquad (26)$$

As the system state variables and their derivatives are bounded, define a non-negative continuous function η such that $\left|\dot{\bar{\alpha}}_1\right| \le \eta$.

$$L\dot{L} = L\dot{\bar{\alpha}}_1 - \frac{L^2}{\tau} \le L|\eta| - \frac{L^2}{\tau} \qquad (27)$$

Define the tracking error variable of the second subsystem as

$$e_2 = \gamma - \alpha_1 \qquad (28)$$

Substituting Eq. (28) into Eq. (22)

$$\dot{e}_1 = e_2 + \alpha_1 - \dot{Q}_d = -c_1 e_1 + e_2 \qquad (29)$$

In the first subsystem, derive the Lyapunov function:

$$V_1 = \frac{1}{2}e_1^2 + \frac{1}{2}L^2 \qquad (30)$$

The derivative of V_1 is as follows:

$$\dot{V}_1 = e_1\dot{e}_1 + L\dot{L} = -c_1 e_1^2 + e_1 e_2 + L\dot{\bar{\alpha}}_1 - \frac{L^2}{\tau} \qquad (31)$$

From the Young's inequality,

$$L|\eta| = \sqrt{2}L \cdot \frac{1}{\sqrt{2}}|\eta| \le L^2 + \frac{\eta^2}{4} \qquad (32)$$

Substituting Eq. (32) into Eq. (31) yields

$$\dot{V}_1 \le -c_1 e_1^2 + e_1 e_2 + L|\eta| - \frac{L^2}{\tau}$$
$$\le -c_1 e_1^2 + e_1 e_2 + L^2 + \frac{\eta^2}{4} - \frac{L^2}{\tau} \qquad (33)$$

If the design of step 2 allows e_2 converges to 0, then there is

$$\begin{cases} \dot{V}_1 \le -kV_1 + c \\ k = 2\min\left\{-c_1, 1 - \frac{1}{\tau}\right\} \\ c = \frac{\eta^2}{4} \end{cases} \qquad (34)$$

According to Lemma 1 and Eq. (34)

$$0 \le V_1(t) \le \frac{c}{k} + \left[V_1(0) - \frac{c}{k}\right]e^{-kt} \le \frac{c}{k} + V_1(0), \quad \forall t \ge 0 \qquad (35)$$

The above equation shows that V_1 and $\dot{V}_1$ are both bounded, and $\lim\limits_{t\to\infty} V_1 = \frac{c}{k}$.

When e_2 converges to zero, the system state meet half global bounded consistency conditions, 1 stable subsystems, and the system tracking error convergence, $e\to 0$, $Q\to Q_d$

The following fast terminal sliding-mode is selected.

$$s_1 = x + \alpha x^{\lambda} + \beta \dot{x}^{\varepsilon} \qquad (36)$$

where $\lambda=k/h$, $\varepsilon=p/q$, k, h, p, q are all positive odd, and $1<\varepsilon<2$, $\lambda>\varepsilon$, α and β are positive constants.

Drawing on the idea of integral sliding mode, let $x = \int_0^t e_2 d\tau$, then Eq. (36) will be

$$s_1 = \int_0^t e_2 d\tau + \alpha\left(\int_0^t e_2 d\tau\right)^{\lambda} + \beta e_2^{\varepsilon} \qquad (37)$$

The derivative of s_1 is

$$\begin{aligned}\dot{s}_1 &= e_2 + \lambda\alpha\left(\int_0^t e_2 d\tau\right)^{\lambda-1}e_2 + \varepsilon\beta e_2^{\varepsilon-1}\dot{e}_2 \\ &= e_2 + \lambda\alpha\left(\int_0^t e_2 d\tau\right)^{\lambda-1}e_2 + \varepsilon\beta e_2^{\varepsilon-1}(f(\gamma,a,b) + bu_{n2} + \omega - \dot{\alpha}_1)\end{aligned} \qquad (38)$$

Define approaching law as

$$\dot{s}_1 = -\kappa(\xi s_1^{m/n} + \sigma s_1) \qquad (39)$$

where $\kappa = \beta\varepsilon e_2^{\varepsilon-1}$, m and n are positive odd $0<m/n<1$, $\xi >0$, $\sigma >0$.

Let Eq. (38) equals Eq. (39) gives the control law as follows:

$$u_{n2} = -\frac{1}{b}\left[\begin{array}{l}\frac{1}{\lambda\beta}\left(e_2^{2-\varepsilon} + \lambda\alpha\left(\int_0^t e_2 d\tau\right)^{\lambda-1}e_2^{2-\varepsilon}\right) \\ +\xi s^{m/n} + \sigma s + f(\gamma,a,b) + \omega(t) - \dot{\alpha}_1\end{array}\right] \qquad (40)$$

The ESO is used for real-time observation of the total internal and external disturbances of the system, $z_3 = f(\gamma, a, b) + \omega(t)$, with dynamic compensation in the control law section.

$$\begin{cases} u_{n2} = u_0 + u_1 \\ u_0 = -\dfrac{1}{b}\left[\dfrac{1}{\lambda\beta}(e_2^{2-\varepsilon} + \lambda\alpha(\int_0^t e_2 d\tau)^{\lambda-1} e_2^{2-\varepsilon}) + \xi s^{m/n} + \sigma s \right] \\ u_1 = z_3 - \dot\alpha_1 \end{cases} \quad (41)$$

Define the Lyapunov function for the second subsystem

$$\begin{aligned} \dot V_2 &= s_1 \dot s_1 \\ &= s_1\left[-\kappa(\xi s_1^{m/n} + \sigma s_1) \right] \\ &= -\beta\varepsilon e_2^{\varepsilon-1}(\xi s_1^{m/n+1} + \sigma s_1^2) \end{aligned} \quad (42)$$

When $s_2 \neq 0$, $\varepsilon = p/q$, $0 < m/n < 1$, $1 < p/q < 2$. Since p, q, m, and n are positive odd numbers, $e_1 > 0$, $s^{m/n}+1 > 0$, then $V_1 \leqslant 0$. From Lyapunov's theorem, we can get that the system will be stable and the state error $e_2 \to 0$ in a certain time. When e_2 converges to 0, Eq. (34) holds, and the whole closed-loop system is bounded and stable in all states.

4 RESULTS AND DISCUSSIONS

To verify the validity of the proposed fuel flow control strategy, simulations are conducted based on the fuel supply demand of a small-thrust turbofan engine.

The fuel flow and rotation speed response of the pump are shown in Figure 4. With the delivery pressure of 6 MPa, Figure 4(a) depicts several typical responses to the flow rate command. The flow command steps from 30 L/min to 45 L/min at 0.2 s and then step back to 35 L/min at 0.4 s is given. For each control method, the fuel flow can be controlled at its required value. However, the system with hybrid control lasts for less than 0.1 s to reach the steady state, and the settling time is only 53% of the system using ADRC, with a smaller overshoot compared to SMC. Figure 4(a) illustrates the flow fluctuation for the command of 45 L/min. The flow rate undulates from 44.8 L/min to 45.2 L/min, at a frequency of about 450 Hz, which is consistent with the theoretical value of the gear pump. The pump system with the proposed control strategy exhibits a fast increase in speed,

creating the condition for the pump to reach the desired flow rate faster.
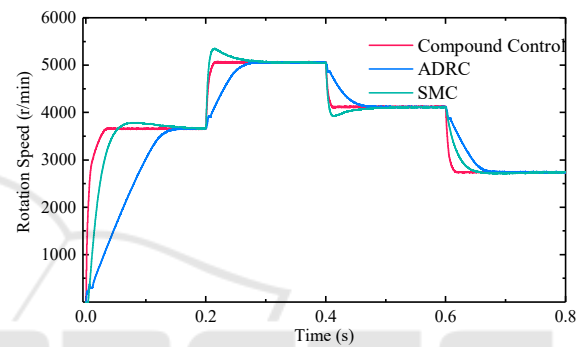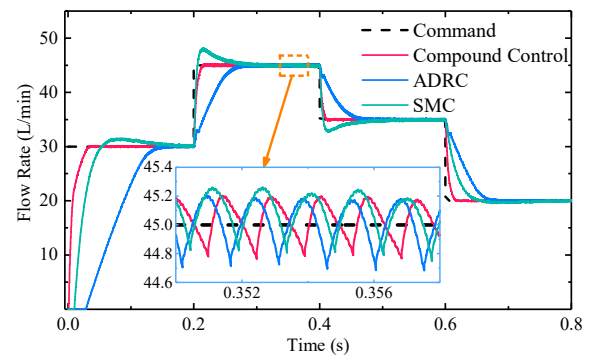
(a) Flow rate

(b) Rotation speed

Figure 4: Pump responses under a step command.

Delivery pressure of the electric fuel pump is easily affected by airborne fuel pipeline or a combustor of the engine. It is a leading factor that adds an obstacle on the flow control. Thus, an important performance of the electric fuel pump is the ability to suppress disturbances, such as the delivery pressure. In order to find a comprehensive superior method, some simulations are conducted to verify their robustness and anti-interference performance. Under any conditions, the fuel supply must be adequate for the engine. For that reason, the constant flow command of 30 L/min, as well as the varying the delivery pressure at the outlet of the pump, is simulated. As shown in Figure 5, the output pressure step from 6 MPa to 7 MPa is given, following an opposite step to the initial. The flow rate plunges instantly when the delivery pressure lifts. Since the command remains constant, the controller needs to compensate for the flow loss due to leakage by increasing the speed output. An ever-rising differential pressure is responsible for the increasing

leakage. Likewise, the flow rate reduces in response to a drop in the pressure by adjusting the output of the speed controller, so that the flow rate can keep very close to the command. The system with hybrid control exhibits faster response and smaller error rate, so better robustness and stronger interference resistance is verified.

As shown in Figure 6(a) and Figure 6(b), an open circuit fault occurred in the UVW phase winding at the moment of 0.06 s. The motor speed decreased instantaneously by about 280 r/min, and then stabilized within 2 ms. The flow rate is reduced by about 3 L/min due to the sudden drop in rotation speed, and then stabilizes with the speed. Figure 28 shows that the speed control stability is good, fluctuating about 8%, and the fault state adjustment time is less than 2 ms, which effectively realizes the fault tolerance function of the system. Figure 6(c) to Figure 6(f) shows the response of the motor. Before an open-circuit fault occurs, each set of windings takes 50% of the power each with a peak current of

16 A. When an open-circuit fault occurs in the U-phase winding, the current in each phase of the UVW set of windings is zero, while the current in each phase of the ABC set of the other normal winding is doubled with a peak current of 32 A each. The ABC windings takes 100% of the power to ensure that the system output power remains unchanged. Figure 6(c) shows the torque waveform generated by the normal set of motor winding ABC, and Figure 6(d) shows the total electromagnetic torque waveform of the motor. The figure shows that the output torque of the normal phase winding ABC is half of the rated load before the fault. When the fault occurs, as the fault phase winding UVW no longer provides output power, the ABC winding will output the entire rated load power and the output torque doubles to 10 N·m. The total electromagnetic torque of the motor is stable around 10 N·m before and after the open-circuit fault of the U-phase winding. The torque is basically unchanged before and after the open-circuit fault.
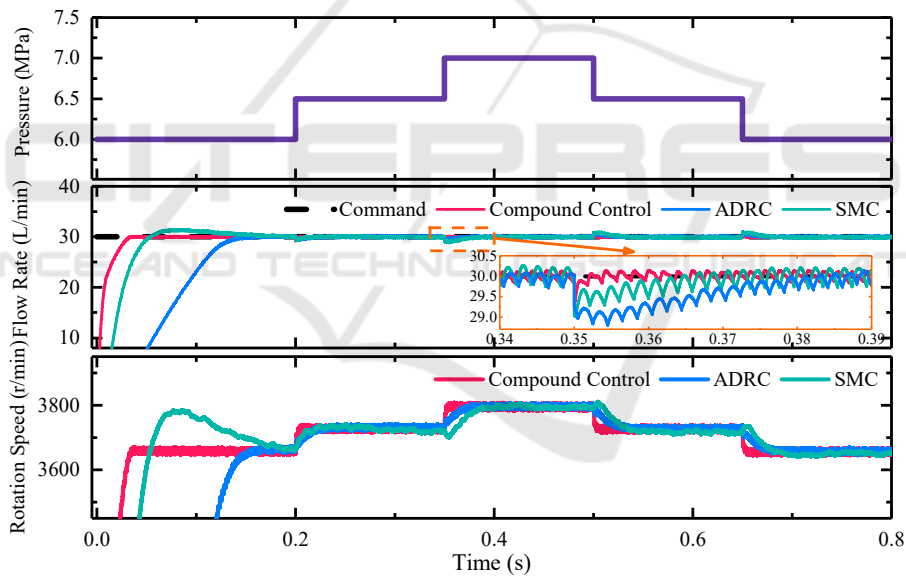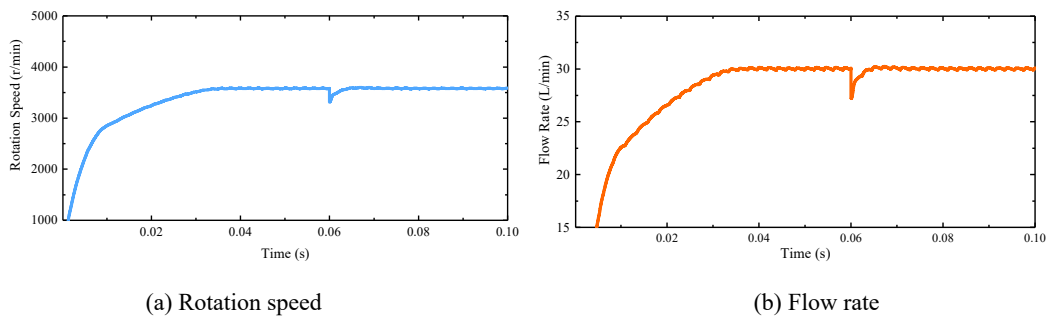
Figure 5: Flow rate under disturbance.

(a) Rotation speed

(b) Flow rate

(c) Current of phase ABC

(d) Current of phase UVW

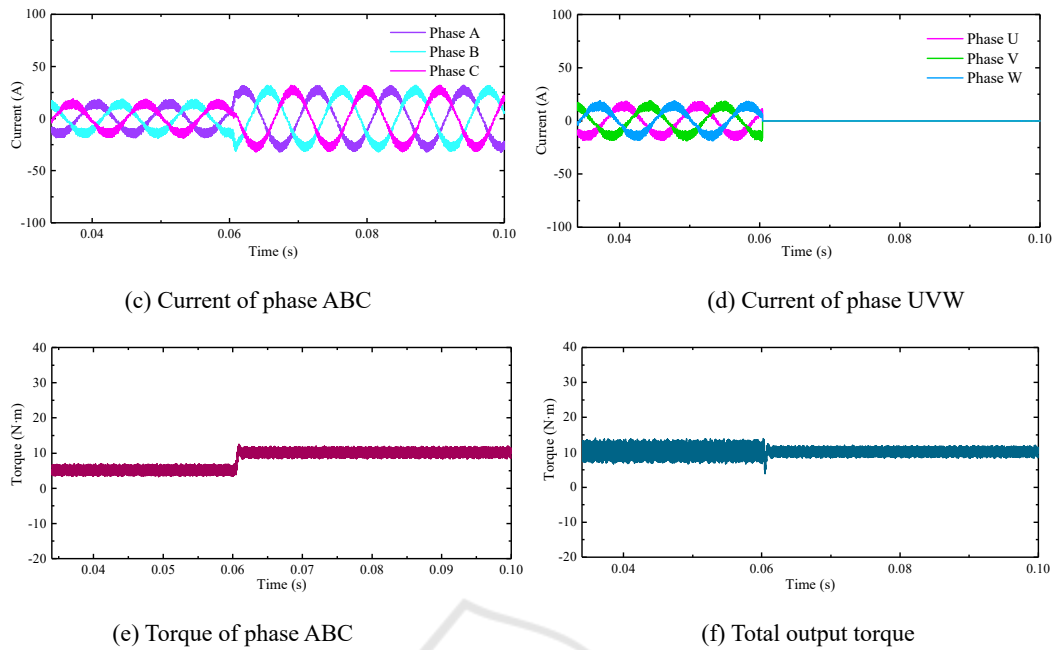(e) Torque of phase ABC

(f) Total output torque

Figure 6: Response with Open Circuit Fault.

5 CONCLUSIONS

To achieve accurate flow control of an electric fuel pump, this paper has proposed a hybrid control strategy. A PMSM and a gear pump are mathematically modelled, and simulations with the proposed control strategy have been carried out under typical conditions. The results are analysed and compared with the results of using ADRC and SMC. The main conclusions are drawn as the following:

(1) With the consideration of instantaneous flow rate, internal leakage and dynamic torque, a complete mathematical model of an electric fuel pump has been developed.

(2) The proposed hybrid control strategy consists of a feed-forward compensation based on differential pressure and backstepping non-singular fast terminal sliding mode control with extend state observer. It can reduce the flow response time and bring about a negligible error of steady-state error, compared with the system using ADRC and SMC. When there exists pressure fluctuation at the pump outlet, the proposed control method exhibits better anti-interference ability including less than 0.5% of steady-state error of the system output.

(3) Considering the possible fault of the motor during the operation of the electric fuel pump, the simulation of the motor open circuit fault was carried out. Results show that the fault state adjustment time is less than 2 ms, and the total torque is basically unchanged before and after the open-circuit fault occurs.

ACKNOWLEDGEMENTS

REFERENCES

Ding R, Xiao L, Jin X. Robust Control for Electric Fuel Pump with Variant Nonlinear Loads Based on a New Combined Sliding Mode Surface[J]. International Journal of Control Automation and Systems, 2019, 17(3):716-728.

Jiang X, Huang W, Cao R, et al. Electric Drive System of Dual-Winding Fault-Tolerant Permanent-Magnet Motor for Aerospace Applications[J]. IEEE

Transactions on Industrial Electronics, 2015, 62(12):7322-7330.

J.Q. Han, From PID Technique to Active Disturbances Rejection Control Technique, Basic Auto-motion, (2002).

K. Chen, L.F. Qian, Y.U. Xiao-Peng, H.M. Zheng, X. Fang, Research on random internal leakage model for external gear pumps, Chinese Journal of Computational Mechanics, (2018). (In Chinese)

Liu, Zhongqiang, et al. "Application of Improved BP Neural Network to the Modeling of Electric Gear Pump." International conference on Big Data Analytics for Cyber-Physical-Systems. Springer, Singapore, 2020.

McLoughlin Adam, Rolls-Royce plc, "Engine Powerplant Electrical Systems", More Electric Aircraft Forum, 2009.

Mohammadi S J, Miran Fashandi S A, Jafari S, et al. A scientometric analysis and critical review of gas turbine aero-engines control: From Whittle engine to more-electric propulsion[J]. Measurement and Control, 2021, 54(5-6): 935-966.

Morioka N, Oyori H, Gonda Y, et al. Development of the Electric Fuel System for the More Electric Engine[C]//ASME Turbo Expo: Turbine Technical Conference & Exposition. American Society of Mechanical Engineers, 2014.

M. Rundo, Models for Flow Rate Simulation in Gear Pumps: A Review[J]. Energies, 2017, 10(9): 1261.

Newman, R., "The More Electric Engine Concept," SAE Technical Paper 2004-01-3128, 2004.

N. Morioka, H. Oyori, More Electric Architecture for Engine and Aircraft Fuel System, Sae Technical Papers, 8 (2013).

X. Wang, J. Atkin, C. Hill, S. Bozhko, Power Allocation and Generator Sizing Optimisation of More-Electric Aircraft On-board Electrical Power during Different Flight Stages, AIAA Propulsion and Energy 2019 Forum, 2019.

Y. Li, Liu, Dynamic Reappearance on Torque Calculation in a Gear Pump with External Mesh, Transactions of the Chinese Society for Agricultural Machinery, (2006). (In Chinese).

Z. Gao, Scaling and bandwidth-parameterization based controller tuning, IEEE, 2003.